6-Chloro-5-[4-(1-Hydroxycyclobutyl)Phenyl]-1H-Indole-3-Carboxylic Acid is a Highly Selective Substrate for Glucuronidation by UGT1A1, Relative to β-Estradiol

Kimberly Lapham, Jian Lin, Jonathan Novak, Christine Orozco, Mark Niosi, Li Di,
Theunis C. Goosen, Sangwoo Ryu, Keith Riccardi, Heather Eng, Kimberly O. Cameron,
and ⓘDAmit S. Kalgutkar

Medicine Design, Pfizer Inc., Groton, Connecticut (K.L., J.L., J.N., C.O., M.N., L.D., T.C.G., S.R., K.R., H.E.); and Medicine Design, Pfizer Inc., Cambridge, Massachusetts (K.O.C., A.S.K.)

ABSTRACT

6-Chloro-5-[4-(1-hydroxycyclobutyl)phenyl]-1H-indole-3-carboxylic acid (PF-06409577) is a direct activator of the human β1-containing adenosine monophosphate-activated protein kinase (AMPK) isoforms. The clearance mechanism of PF-06409577 in animals and humans involves uridine diphosphoglucuronosyl transferase (UGT)–mediated glucuronidation to an acyl glucuronide metabolite of PF-06409577 [(2S,3S,4S,5R,6S)-6-((6-chloro-5-(4-(1-hydroxycyclobutyl)phenyl)-1H-indole-3-carbonyl)oxy)-3,4,5-trihydroxytetrahydro-2H-pyran-2-carboxylic acid (M1)], which retains selective activation of human β1-containing AMPK isoforms. This paper describes a detailed characterization of the human UGT isoform(s) responsible for glucuronidation of PF-06409577 to M1. Studies using a panel of 13 human recombinant UGT (hrUGT) enzymes indicated that PF-06409577 was converted to M1 in a highly selective fashion by UGT1A1, which was further verified in human liver microsomes treated with specific chemical inhibitors, and in different UGT1A1 expressers. Conversion of PF-06409577 to M1 by UGT1A1 occurred in a relatively selective fashion, compared with β-estradiol (ES), a conventional probe substrate of UGT1A1. The Michaelis-Menten constant (K_M) and V_{max} values describing the formation of M1 from PF-06409577 in hrUGT1A1 and microsomal preparations from human intestine, liver, and kidney ranged from 131 to 212 μM (K_M) and 107–3834 pmol/min per milligram (V_{max}) in the presence of 2% bovine serum albumin. Relative activity factors (RAF) were determined for UGT1A1 using PF-06409577 and ES to enable estimation of intrinsic clearance from various tissues. RAF values from PF-06409577 and ES were generally comparable with the exception of intestinal microsomes, where ES overestimated the RAF of UGT1A1 due to glucuronidation by intestinal UGT1A8 and UGT1A10. Our results suggest the potential utility of PF-06409477 as a selective probe UGT1A1 substrate for UGT reaction phenotyping and inhibition studies in preclinical discovery/development.

Introduction

A recent paper from our laboratory (Cameron et al., 2016) reported structure-activity relationship studies on a series of indole-3-carboxylic acid derivatives as direct activators of human adenosine monophosphate-activated protein kinase (AMPK), a protein kinase involved in maintaining energy homeostasis within cells, which culminated in the discovery of 6-chloro-5-[4-(1-hydroxycyclobutyl)phenyl]-1H-indole-3-carboxylic acid (PF-06409577) (Fig. 1) as a potent, direct, and selective activator of the human α1β1γ1 AMPK isoform. On the basis of its attractive preclinical pharmacokinetics, pharmacodynamics, and safety, PF-06409577 has been advanced into first-in-human clinical trials for the potential treatment of diabetic nephropathy. The metabolic elimination mechanism of

PF-06409577 in animals and humans involves glucuronidation by a uridine diphosphoglucuronosyl transferase (UGT) isoform(s) (Cameron et al., 2016). PF-06409577 is resistant toward oxidative modifications by cytochrome P450 enzymes in liver microsomes and/or hepatocytes from preclinical species and human. Recently, we described the biosynthetic preparation, purification, and structural characterization of the glucuronide conjugate of PF-06409577—(2S,3S,4S,5R,6S)-6-((6-chloro-5-(4-(1-hydroxycyclobutyl)-phenyl)-1H-indole-3-carbonyl)oxy)-3,4,5-trihydroxytetrahydro-2H-pyran-2-carboxylic acid (M1)—obtained from incubations of the parent compound in uridine 5'-diphosphoglucuronic acid (UDPGA)–supplemented human liver microsomes (HLM) (Ryder et al., 2018). A combination of chemical derivatization and spectral characterization studies on purified M1 indicated that the metabolite was derived from the glucuronidation of the carboxylic acid moiety in PF-06409577 (Fig. 1). In vitro pharmacological evaluation utilizing a time-resolved fluorescence resonance energy transfer activation/protection assay

ABBREVIATIONS: AMPK, adenosine monophosphate-activated protein kinase; AZT, zidovudine; BSA, bovine serum albumin; CL$_{int}$, intrinsic clearance; CL$_{int,u}$, unbound intrinsic clearance; DMSO, dimethylsulfoxide; ES, β-estradiol; ES-3-G, β-estradiol-3-glucuronide; HIM, human intestinal microsomes; HKM, human kidney microsomes; HLM, human liver microsomes; hrUGT, human recombinant UGT; IS, internal standard; K_M, Michaelis-Menten constant; LC-MS/MS, liquid chromatography–tandem mass spectrometry; M1, (2S,3S,4S,5R,6S)-6-((6-chloro-5-(4-(1-hydroxycyclobutyl)phenyl)-1H-indole-3-carbonyl)oxy)-3,4,5-trihydroxytetrahydro-2H-pyran-2-carboxylic acid; PF-06409577, 6-chloro-5-[4-(1-hydroxycyclobutyl)phenyl]-1H-indole-3-carboxylic acid; RAF, relative activity factor; UDPGA, uridine 5'-diphosphoglucuronic acid; UGT, uridine diphosphoglucuronosyl transferase.
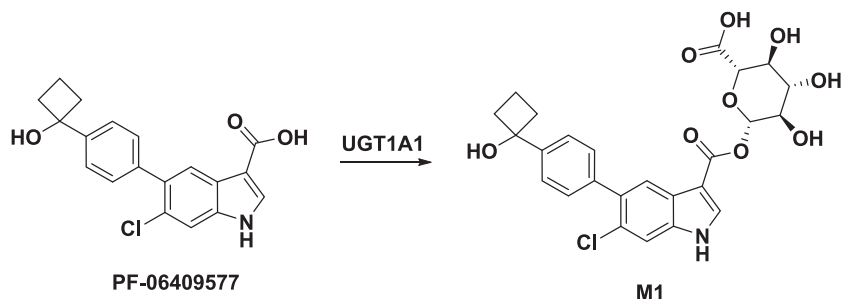
Fig. 1. Conversion of PF-06409577 to M1 by UGT1A1.

revealed that M1 was an active metabolite, and retained selective activation of the human β1-containing AMPK isoforms. Cocrystallization of the human AMPK α1β1γ1 isoform with PF-06409577 and M1 provided molecular insights into the structural basis for AMPK activation by the phase 2 conjugation product (Ryder et al., 2018).

Mammalian UGTs comprise a superfamily of endoplasmic reticulum membrane–bound enzymes, which are expressed in liver and extrahepatic tissues such as small intestine, kidney, brain, skin, breast, uterus, and prostate (Mackenzie et al., 1997; Tukey and Strassburg, 2000, 2001; Fisher et al., 2001; Hu et al., 2014). UGTs primarily catalyze the covalent adduction of glucuronic acid, derived from the cofactor UDPGA, to structurally diverse nucleophilic substrates (e.g., phenols, alcohols, amines, thiols, and carboxylic acids) (Miners and Mackenzie, 1991; Hawes, 1998; Sakaguchi et al., 2004; Kaivosaari et al., 2011; Argikar, 2012). Compared with the plethora of clinically relevant drug-drug interactions arising via inhibition or induction of cytochrome P450 enzyme activities, drug-drug interaction risks due to the inhibition or induction of human UGTs are considered to be relatively low (Kiang et al., 2005; Devineni et al., 2015; Krishna et al., 2016). Likewise, clinically relevant examples that require dose adjustment for a poor UGT-metabolizer genotype are rare, except for reports on some UGT1A1 substrates (Toffoli et al., 2006; Court, 2010). Nevertheless, a thorough evaluation of the potential for UGT drug-drug interactions, both as perpetrator and victim, needs to be considered when developing new chemical entities, as highlighted in recent reviews on this topic (Bjornsson et al., 2003; Zhang et al., 2010).

The present article summarizes our efforts toward reaction phenotyping studies aimed at identifying the UGTs responsible for conversion of PF-06409577 to M1. Incubation of PF-06409577 with 13 individual human recombinant UGTs (hrUGTs) revealed that metabolism of PF-06409577 to M1 was selectively catalyzed by polymorphic UGT1A1 (Beutler et al., 1998; Duguay et al., 2004; Sai et al., 2004; Sugatani, 2013). Significant impairment of the glucuronidation of PF-06409577 in UDPGA-supplemented HLM pretreated with specific UGT1A1 inhibitors or in HLM possessing UGT1A1*1/*28 or UGT1A1*28/*28 genetic mutations in the promoter region of UGT1A1, polymorphisms that correspond to reduced enzyme activity, further confirmed the selective role of this isozyme in the formation of M1. PF-06409577 was found to be considerably more selective as a UGT1A1 substrate in comparison with the prototypic UGT1A1 probe substrate β-estradiol (ES) used in UGT inhibition studies. The kinetic parameters (V_{max}, i.e., the maximum rate of glucuronidation) and the Michaelis-Menten constant (K_M) for the conversion of PF-06409577 to M1 were obtained with hrUGT1A1 and microsomal preparations obtained from human intestine, liver, and kidney, which are known to express UGT1A1 protein (Ohno and Nakajin, 2009; Harbourt et al., 2012; Fujiwara et al., 2015). UGT1A1 relative activity factor (RAF) values determined with PF-06409577 were similar to ES in all tissues except microsomal preparations from human small intestine. In addition to UGT1A1, the conversion of ES to β-estradiol-3-glucuronide (ES-3-G)

was catalyzed by UGT1A3 and intestine-specific UGT1A8 and 1A10 isoforms (Tukey and Strassburg, 2001), whereas PF-06409577 was not a substrate for UGT1A3, 1A8, and 1A10. Overall, our results suggest that PF-06409477 is a significantly more selective UGT1A1 probe substrate compared with ES.

Materials and Methods

Materials. The synthesis of compound PF-06409577 (chemical purity >99% by high-performance liquid chromatography and NMR) has been previously reported (Cameron et al., 2016). PF-06409577 is commercially available from Sigma Aldrich (St. Louis, MO). The biosynthetic methodology (scale-up of UDPGA-supplemented HLM incubations of PF-06409577) for preparation of the acyl glucuronide M1 has been previously described (Ryder et al., 2018). Examination of the degradation kinetics of the biochemically isolated M1 in deuterated phosphate buffer (pH ~7.4) at 37°C using a NMR method developed to monitor the disappearance of the anomeric proton (δ~5.7–5.8 ppm) in β-O-1-acyl glucuronides revealed that M1 was inert toward hydrolysis or acyl migration (half-life > 21 hours) (Ryder et al., 2018). As a general precaution, solid material corresponding to parent (PF-06409577) and acyl glucuronide (M1) was stored in sealed vials under argon. Stock solutions of PF-06409577 and M1 were freshly prepared in dimethylsulfoxide (DMSO) for each experiment, since long-term storage (>7 days) of the DMSO stock solutions of PF-06409577 and M1 can result in compound degradation (dehydration in PF-06409577 and hydrolysis of M1 to PF-06409577) to some degree (2% to 3%). Alamethicin, UDPGA trisodium salt, trizma hydrochloride, ES, ES-3-G, diclofenac, digoxin, zidovudine (AZT), propofol, 1 M potassium phosphate dibasic solution, 1 M potassium phosphate monobasic solution, bovine serum albumin [(BSA), product A7906], and DMSO were purchased from Sigma Aldrich. Alamethicin, UDPGA trisodium salt, trizma hydrochloride, ES, ES-3-G, diclofenac, digoxin, AZT, propofol, 1 M potassium phosphate dibasic solution, 1 M potassium phosphate monobasic solution, BSA (product A7906), and DMSO were purchased from Sigma Aldrich. Atazanavir and 1-napthyl-glucuronide were purchased from Sequoia Research Products (Pangbourne, United Kingdom). Zidovudine-5′-glucuronide, [^{13}C$_6$]zidovudine-5′-glucuronide, 5-hydroxytryptophol, propofol-O-glucuronide, trifluoperazine-N-glucuronide, and [D$_3$]trifluoperazine-N-glucuronide were purchased from Cerilliant (Austin, TX). 5-Hydroxytryptophol-glucuronide was obtained by biosynthesis as detailed in Walsky et al. (2012). Pooled HLM prepared from 50 mixed-gender donors (20.0 mg of microsomal protein/ml or 0.302 nmol of total UGT/mg of microsomal protein, 43.6 pmol of total UGT1A1/mg of microsomal protein) were obtained from BD Gentest (Woburn, MA). cDNA-expressed hrUGTs were procured from BD Gentest. The following hrUGT enzymes were used in the activity screening studies: UGT1A1, UGT1A3, UGT1A4, UGT1A6, UGT1A7, UGT1A8, UGT1A9, UGT1A10, UGT2B4, UGT2B7, UGT2B10, UGT2B15, and UGT2B17, and also a nonactive UGT control protein was used to provide a uniform protein concentration among UGT incubation reactions. Genotyped HLM obtained from BD Gentest were pooled from five donors as follows: UGT1A1 *1/*1 HH2 (Caucasian male), HH74 (Caucasian male), HH75 (Caucasian male), HH88 (Caucasian female), HH110 (Caucasian female); UGT1A1 *1/*28 HH41 (Caucasian female), HH71 (Caucasian male), HH98 (Caucasian male), HH103 (African-American female), HH105 (Caucasian male); and UGT1A1 *28/*28 HH9 (Caucasian male), HH81 (Caucasian male), HH82 (Caucasian female), HH90 (Caucasian male), HH95 (Hispanic male). Pooled male and female human intestinal microsomes (HIM)

and human kidney microsomes (HKM) were purchased from XenoTech (Kansas City, KS).

General UGT Incubation Conditions. The specifics of each incubation condition are described in the individual sections but, in general, incubations were conducted using the conditions described herein. Microsomes (HLM, HIM, HKM, or hrUGTs) were mixed with 100 mM Tris-HCl buffer (pH 7.5 at 37°C) containing 5 mM magnesium chloride, substrates, and 2% BSA unless otherwise noted. Incubation mixtures were preincubated with 10 μg/ml alamethicin on ice for 15 minutes to enable pore formation (Walsky et al., 2012). Following 5-minute preincubation at 37°C, the reactions were initiated with addition of 5 mM UDPGA. At predetermined time points, the incubations were terminated with acetonitrile containing internal standard [(IS), 0.6 μM diclofenac for PF-06409577; 1 μM diclofenac for ES]. Solutions were centrifuged (1900g), and the supernatants were analyzed by liquid chromatography–tandem mass spectrometry (LC-MS/MS) and quantified against a standard curve (M1 for PF-06409577; ES-3-G for ES).

Reaction Phenotyping with hrUGT Isoforms in the Absence of BSA. In a preliminary UGT reaction phenotyping study, PF-06409577 (5 μM) was incubated in duplicate with 13 hrUGTs (1A1, 1A3, 1A4, 1A6, 1A7, 1A8, 1A9, 1A10, 2B4, 2B7, 2B10, 2B15, and 2B17) and UGT vector control at 0.5 mg/ml protein concentration. Periodically, aliquots of the incubation mixture were quenched with acetonitrile containing IS. Samples were analyzed by LC-MS/MS for disappearance of PF-06409577 by area ratio. To further confirm selectivity, PF-06409577 (2.40, 24.0, and 240 μM) was incubated in duplicate with the same 13 hrUGTs and vector control (0.25 mg/ml protein concentration). At 60 minutes, an aliquot of the incubation mixture was quenched with IS. The samples were quantified by LC-MS/MS against a M1 standard curve. Similar to PF-06409577, UGT reaction phenotyping of ES (3.34, 33.4, and 334 μM) was incubated in triplicate with 13 hrUGTs and UGT vector control (0.025 mg/ml). At 60 minutes, an aliquot of the incubation mixture was quenched with acetonitrile containing IS. Samples were quantified by LC-MS/MS against an ES-3-G standard curve.

Enzyme Kinetics of PF-06409577 in HLM and ES in hrUGT1A1 in the Absence of BSA. Under linear conditions (with respect to protein concentration and time), the V_{max} and K_M values were determined in triplicate using 12 substrate concentrations (5–500 μM for PF-06409577; 1–1000 μM for ES) in HLM (0.25 mg/ml) for PF-06409577 and hrUGT1A1 (0.25 mg/ml) for ES. Following 60-minute incubation, aliquots of the incubation were quenched with acetonitrile containing IS. The supernatants were analzyed by LC-MS/MS for metabolite formation (M1 or ES-3-G) with appropriate standard curves. Data were used to select concentrations in the hrUGT phenotyping screen.

Enzyme Kinetics of PF-06409577 and ES in HLM, HIM, HKM, and hrUGT1A1 in the Presence of BSA. The linearity of M1 and ES-3-G formation with respect to time and protein concentration were conducted with UDPGA-supplemented HLM, HIM, HKM, and hrUGT1A1 in the presence of 2% BSA. Under linear conditions, the V_{max} and K_M values were determined in replicates of two or three using 12 substrate concentrations (1–1000 μM for PF-06409577; 1–1000 μM for ES) in HLM, HIM, HKM, or hrUGT1A1 (0.25 mg/ml for PF-06409577; 0.025 mg/ml for ES). Following 30-minute incubation, aliquots were quenched with acetonitrile containing IS. The supernatants were analzyed by LC-MS/MS for metabolite formation (M1 or ES-3-G) with appropriate standard curves.

Chemical Inhibition Study in HLM in the Presence of BSA. UGT isoform–selective chemical inhibitor experiments were performed in triplicate. PF-06409577 was incubated at a concentration approximating 1/200th of the apparent K_M value (1 μM), with pooled UGT1A1*1/*1 wild-type, heterozygote

*1/*28, and homozygote *28/*28 HLM (0.025 mg/ml) in the presence of 2% BSA, UGT1A1 inhibitor atazanavir (10 μM), UGT1A9 inhibitor digoxin (10 μM), or solvent (DMSO) control. Inhibitor concentrations were selected based on previous studies in our laboratories utilizing isoform-selective probe substrates (Lapham et al., 2012; Walsky et al., 2012). At 30 minutes, aliquots were removed and quenched with acetonitrile containing IS. The samples were quantified by LC-MS/MS against a M1 standard curve. The percentage of inhibition of M1 formation was calculated relative to the control activity for each genotype (*1/*1, *1/*28, and *28/*28).

Inhibition of UGT Isoforms by PF-06409577 and ES in the Absence of BSA. The potential for PF-06409577 (1–100 μM) to inhibit UGT 1A1, 1A4, 1A6, 1A9, and 2B7 enzyme activities was investigated in HLM (0.025 mg/ml) using our previously described methodology (Walsky et al., 2012). The UGT isoform–specific probe substrates are described in Table 1. During the development of an in-house cocktail UGT IC$_{50}$ assay, we discovered that ES inhibited UGT2B7-catalyzed glucuronidation of AZT. To fully characterize the inhibitory effects against UGT2B7, ES (1–100 μM) was incubated in HLM (0.025 mg/ml) in the absence of 2% BSA using our previously described methodology (Walsky et al., 2012).

Determination of Unbound Fraction in Incubations. Binding of PF-06409577 and ES under the in vitro incubation conditions was determined by equilibrium dialysis methods previously described (Di et al., 2012). The resulting unbound fraction in incubation values were used to correct for unbound intrinsic clearance (CL$_{int,u}$).

Calculations of Enzyme Kinetic Parameters. Substrate concentration [S] and metabolite formation velocity (v) data were fitted to appropriate enzyme kinetic models using Sigmaplot least-squares regression analysis (Sigmaplot version 13; Systat Software, Inc., San Jose, CA). Best fit was determined by R^2 goodness of fit, Eadie-Hofstee fit, and visual inspection. The enzyme kinetic parameters were modeled using eqs. 1–3:

$$v = \frac{V_{max} \times [S]}{K_M + [S]} \tag{1}$$

$$v = \frac{V_{max} \times [S]}{K_M + [S] \times \{1 + ([S]/K_i)\}} \tag{2}$$

$$v = \frac{V_{max} \times S^h}{S_{50}^h + S^h} \tag{3}$$

The intrinsic clearance (CL$_{int}$) was calculated using eqs. 4 and 5 and CL$_{int,u}$ was derived using eq. 6. The RAF values were calculated using eq. 7.

$$CL_{int} = \frac{V_{max}}{K_M} \tag{4}$$

$$CL_{int} = \frac{V_{max}}{S_{50}} \times \frac{(h-1)}{h \times (h-1)^{1/h}} \tag{5}$$

$$CL_{int,u} = \frac{CL_{int}}{f_{u,inc}} \tag{6}$$

$$RAF = \frac{CL_{int,u(HLM,HIM,HKM)}}{CL_{int,u,hrUGT1A1}} \tag{7}$$

where $f_{u,inc}$ denotes the unbound fraction in incubation.

Calculation of IC$_{50}$ Values. The percentage of activity remaining was obtained by normalizing the concentration data to the solvent control. When ≥50% inhibition was observed at or below the highest inhibitor

TABLE 1

UGT isoform-specific probe substrates used to assess inhibitory properties of PF-06409577

Assay	UGT1A1	UGT1A4	UGT1A6	UGT1A9	UGT2B7
Substrate	ES	trifluoperazine	5HTOL	propofol	zidovudine
Substrate concentration (μM)	10	40	150	5	300
Incubation time (minutes)	60	30	20	30	60
Analyte	ES-3-G	TFP-G	5HTOL-G	PRO-G	AZT-G
IS	1-naphthyl-O-glucuronide	[D$_3$]-TFP-G	diclofenac	diclofenac	[^{13}C$_6$]-AZT-G

AZT-G, zidovudine-5′-glucuronide; 5HTOL, 5-hydroxytryptophol; 5HTOL-G, 5-hydroxytryptophol-glucuronide; PRO-G, propofol-O-glucuronide; TFP-G, trifluoperazine-N-glucuronide.

concentration (100 μM), the IC$_{50}$ values were generated using GraphPad Prism 5 for Windows (version 5.01; GraphPad Software, La Jolla, CA). Nonlinear regression fitting of the data was done using the log [inhibitor] versus normalized response model using the following four-parameter sigmoidal-logistic IC$_{50}$ equation:

$$Y = 100/(1 + 10^{[(logIC_{50-x}) \times Hill\ slope]}) \quad (8)$$

This model forces the curve to run from 100% down to 0%. The Hill slope was assumed constant at -1.0.

LC-MS/MS Analysis. Concentrations of analytes were determined using LC-MS/MS on a Sciex 4000Qtrap or 5500 LC-MS/MS triple quadrupole mass spectrometer (Sciex, Framingham, MA) equipped with a Waters Acquity UPLC (Waters, Milford, MA). The Waters Acquity autosampler was programmed to inject 10 μl of sample onto a MacMod Halo 2.6 μm C18 30 × 2.1 mm column (MacMod Analytical, Chadds Ford, PA) or a Phenomenex C18 2.6 μm C18 30 × 3.0 mm column (Phenomenex, Torrance, CA) using a mobile phase consisting of high-performance liquid chromatography–grade water containing 0.1% (v/v) formic acid (mobile phase A) and acetonitrile containing 0.1% formic acid (mobile phase B) at a flow rate of 0.4–0.8 ml/min. The following general gradient program was used: initial condition 5% mobile phase B for 0.8 minutes, ramped to 95% mobile phase B over 1 minute, held for 0.5 minutes, and returned to initial conditions for column equilibration. PF-06409577 and M1 were detected using negative electrospray ionization in the multiple reactions monitoring mode, monitoring for mass-to-charge ratio transitions 340.0 → 268.0 and 516.0 → 193.1, respectively. ES-3-G was detected with negative electrospray ionization at mass-to-charge ratio transition 447.2 → 113.2. Diclofenac was monitored using negative electrospray ionization at mass-to-charge ratio transition 294 → 250. Unless specified, analytes were quantified versus a standard curve using Analyst software (version 1.5.2; Sciex, Framingham, MA). Data were fit by least-squares regression of their areas to a weighted linear equation, from which the unknown concentrations were calculated.

Results

UGT Reaction Phenotyping with hrUGTs. Preliminary UGT reaction phenotyping studies examining the metabolic decline of PF-06409577 (5 μM) in 13 hrUGT isoforms (UGT1A1, 1A3, 1A4, 1A6, 1A7, 1A8, 1A9, 1A10, 2B4, 2B7, 2B10, 2B15, and 2B17) revealed that PF-06409577 was metabolically unstable (half-life = 55 minutes) in hrUGT1A1 in a UDPGA-dependent fashion (Fig. 2). In contrast, no metabolic decline of PF-06409577 was noted with the remainder of the 12 hrUGT isoforms (half-life > 360 minutes). To support early reaction phenotyping (and selectivity assessments), kinetic parameters were generated for PF-06409577 in HLM and ES in hrUGT1A1 in the absence of BSA. The K_M value for the glucuronidation of PF-06409577 to M1 was 23.9 ± 3.0 μM in HLM. The corresponding hrUGT1A1 K_M value for ES was 33.4 ± 5.6 μM, which is comparable with the values

reported previously for ES in hrUGT1A1 and HLM (Walsky et al., 2012). To compare the relative selectivity of PF-06409577 and ES as UGT1A1 substrates, metabolite formation rates were measured in 13 hrUGTs for PF-06409577 and ES at concentrations approximating the 0.1-, 1.0-, and 10-fold HLM K_M values for PF-06409577 or the hrUGT1A1 K_M value for ES, and the formation of M1 and ES-3-G was monitored. As seen in Fig. 3, the formation of M1 was mediated in a relatively selective fashion by UGT1A1 across the PF-06409577 concentration range studied. In the case of ES, the formation of ES-3-G was mediated by UGT1A1 and UGT1A3 as well as by UGT1A8 and UGT1A10, which are selectively expressed in the small intestine. These data are qualitative in nature, since the RAF values are not available for all of the UGT isoforms. Therefore, the relative contribution of each UGT to ES-3-G formation in the intestine is currently not known.

PF-06409577 and ES Enzyme Kinetics in hrUGT1A1 and Human Tissue Microsomes and Determination of RAF Values. Considering that human UGT1A1 is expressed in liver, intestine, and kidney (Harbourt et al., 2012), the enzyme kinetic parameters for glucuronidation of PF-06409577 (to M1) and ES (to ES-3-G) were assessed in hrUGT1A1 and microsomes from human liver, intestine, and kidney in the presence of 2% BSA. BSA was included because of its propensity to sequester long-chain unsaturated fatty acids that are released from membranes during the course of an incubation (Engtrakul et al., 2005; Walsky et al., 2012). Long-chain unsaturated fatty acids are potent inhibitors of UGT1A9, UGT2B7, and micro-somal glucuronidation activity, resulting in overestimation of K_M values (Tsoutsikos et al., 2004; Rowland et al., 2007, 2008). The enzyme kinetic parameters of M1 formation from PF-06409577 glucuronidation in HLM, HIM, HKM, and hrUGT1A1 are shown in Fig. 4, A–D, respectively. The K_M, V_{max}, and $CL_{int,u}$ values ranged from 116 to 212 μM, 1077 to 3834 pmol/min per milligram protein, and 9.35 to 154 μl/min per milligram protein, respectively, in human tissue microsomes and hrUGT1A1 (Table 2). The corresponding enzyme kinetic data (K_M, V_{max}, and $CL_{int,u}$) for ES glucuronidation to ES-3-G ranged from 19 to 147 μM, 31 to 7095 pmol/min per milligram protein, and 41 to 5760 μl/min per milligram protein, respectively, in human tissue microsomes and hrUGT1A1 (Table 3).

The RAF approach has been used for scaling enzymatic activities (e.g., CL_{int}) using hrUGT enzymes to HLM or HIM (Rouguieg et al., 2010; Zhu et al., 2012; Gibson et al., 2013). RAFs are defined as the human tissue microsomes/human UGT activity ratio of a particular isoform toward an isoform-selective probe substrate in experiments performed under identical conditions. The corresponding RAF values for PF-06409577 (and ES) in HLM, HIM, and HKM were 0.47 (0.7), 0.12 (30), and 0.061 (0.22), respectively (Tables 2 and 3). The UGT1A1
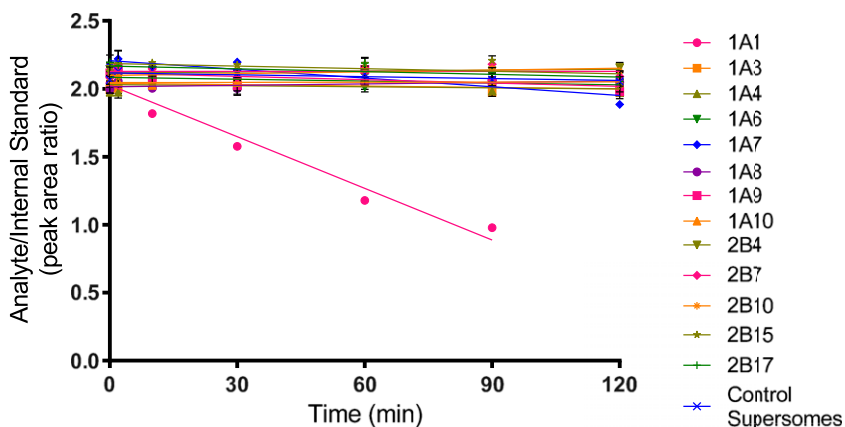

Fig. 2. Metabolic stability of PF-06409577 (5 μM) in 13 hrUGT isoforms (0.5 mg/ml protein concentration) in the presence of UDPGA (5 mM).
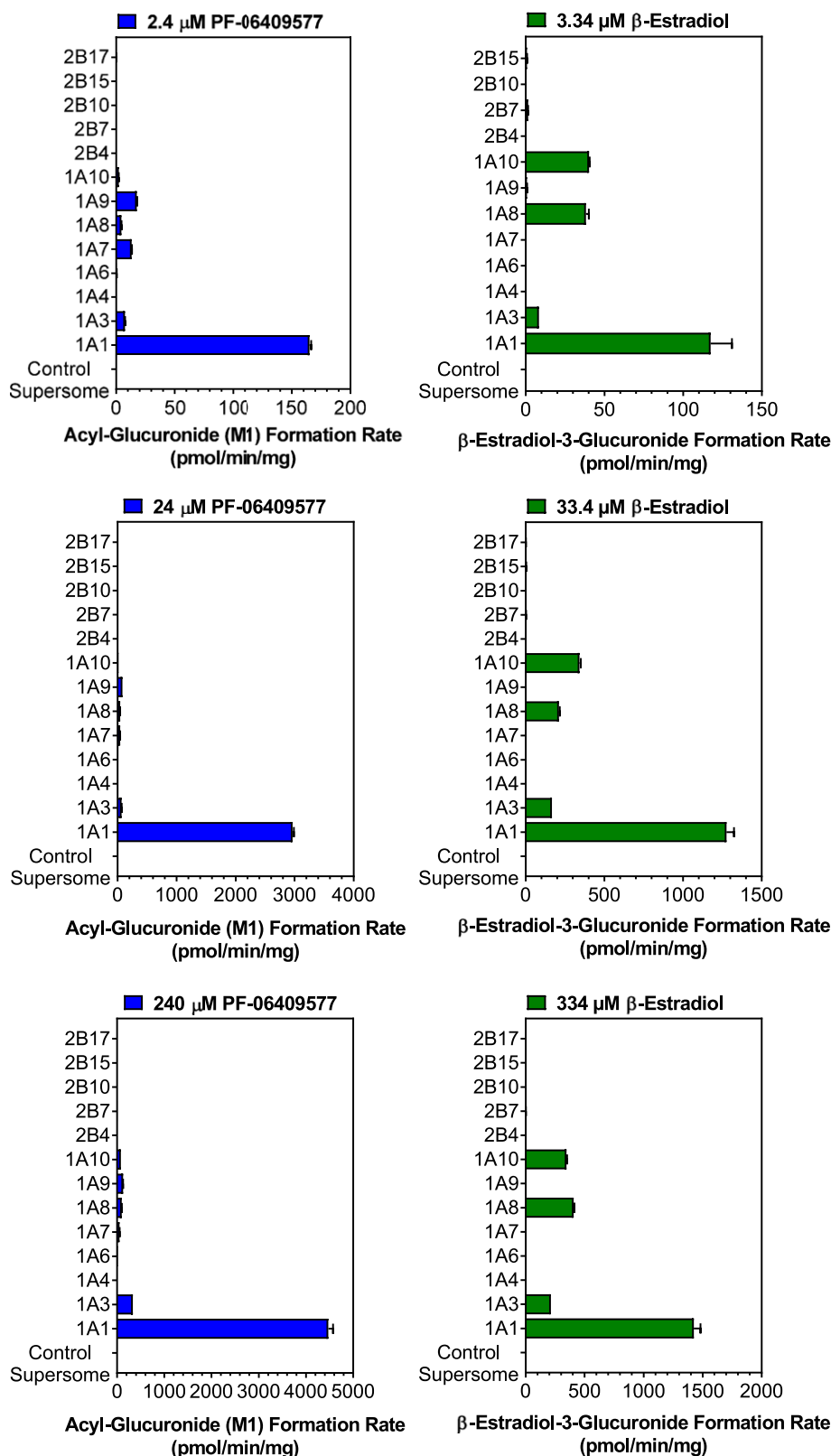
Fig. 3. Selectivity of PF-06409577 (2.4, 24, and 240 μM) and ES (3.34, 33.4, and 334 μM) as UGT1A1 substrates following incubation with 13 hrUGT isoforms. The formation of M1 and ES-3-G was monitored in these experiments.

liver/kidney and liver/intestine abundance ratios were compared with the HLM/HKM and HLM/HIM RAF ratios for PF-06409577 and ES (Fig. 5). UGT1A1 enzyme abundance values were obtained from the simcyp software (Certara, Princeton, NJ): 48, 8.5, and 6.1 pmol/mg protein for liver, intestine, and kidney, respectively. The RAF and UGT1A1 abundance ratios for PF-06409577 were comparable in the target tissues, i.e., RAF HLM/HIM 3.9 versus UGT1A1 abundance liver/intestine 5.7 and RAF HLM/HKM 7.7 versus UGT1A1 abundance liver/kidney 7.9. Although the RAF value of 3.2 for ES in HLM/HKM was comparable with the UGT1A1 liver/kidney abundance (7.9), an approximately 250-fold difference was
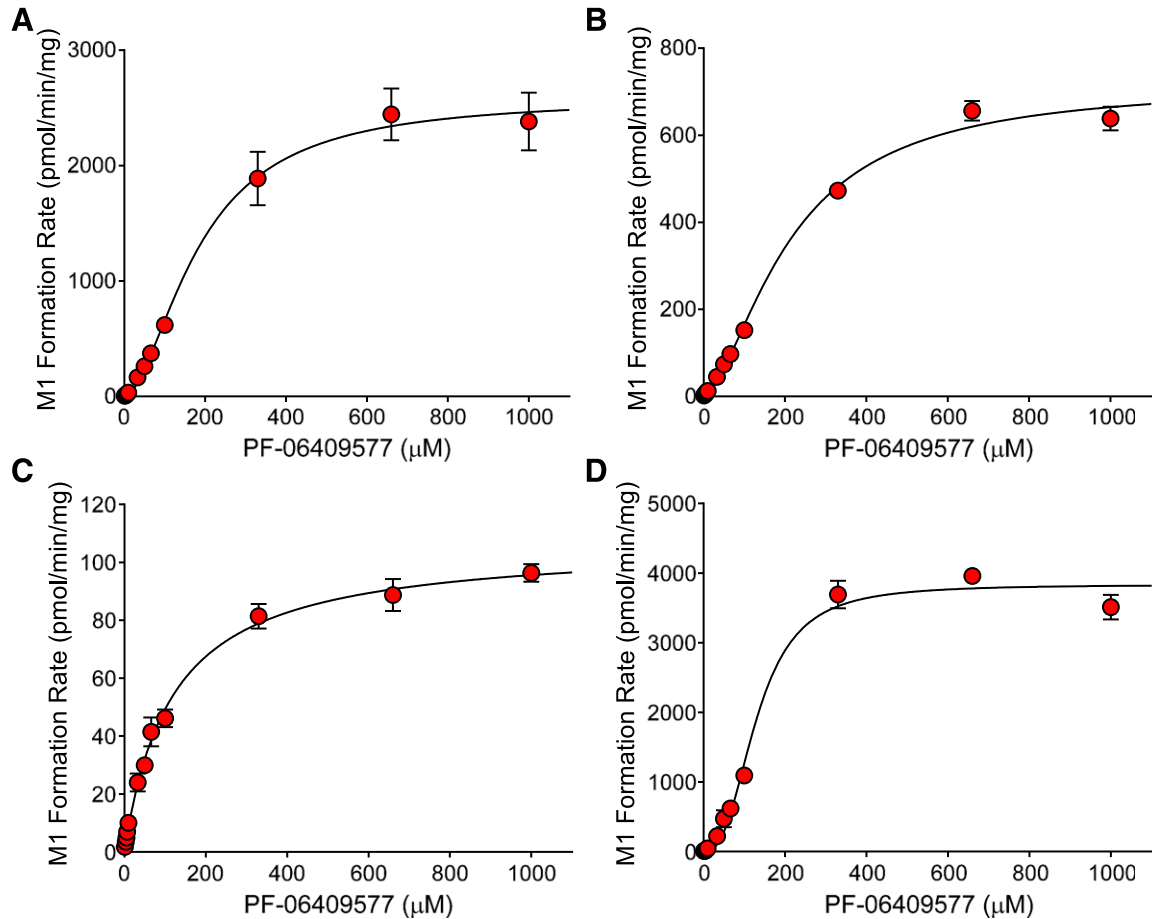
Fig. 4. Enzyme kinetics for the glucuronidation of PF-06409577 to M1 in UDPGA-supplemented HLM (A), HIM (B), HKM (C), and hrUGT1A1 (D). Symbols depict mean values and error bars depict S.D.

noted between the ES RAF value in HLM/HIM (0.023) and the UGT1A1 liver/intestine tissue abundance (5.7).

UGT1A1 Chemical Inhibition Studies in Genotyped HLM. Additional UGT1A1 inhibition studies for PF-06409577 with UGT1A1*28 genotyped HLM indicated approximately ~25% and 74% reductions in the CL$_{int}$ with heterozygous UGT1A1*1/*28 (12.5 μl/min per milligram) and homozygous UGT1A1*28/*28 (4.3 μl/min per milligram), respectively, compared with wild-type UGT1A1*1/*1 HLM (16.6 μl/min per milligram) (Fig. 6) at 1 μM, which approximated ~1/200th of the K_M value for PF-06409577 in HLM. The potent UGT1A1 chemical inhibitor atazanavir (Zhang et al., 2005) at 10 μM inhibited M1 formation by ~98%, 95%, and 90% in UGT1A1*1/*1,

UGT1A1*1/*28, and UGT1A1*28/*28 genotyped HLM (Fig. 7). In contrast, the formation of M1 was only inhibited by 15%, 12%, and 13% in wild-type UGT1A1*1/*1, UGT1A1*1/*28, and UGT1A1*28/*28 HLM in the presence of digoxin (10 μM), which is a potent UGT1A9 (but weak UGT1A1) inhibitor (Lapham et al., 2012).

UGT Inhibition by PF-06409577 and ES in HLM. To compare the utility of PF-06409577 versus ES as UGT1A1 probe substrates in a cocktail UGT inhibition assay in HLM, the potential of PF-06409577 as an inhibitor of the major human UGT isoforms (1A1, 1A4, 1A6, 1A9, and 2B7) was investigated in HLM using our previously described protocol (Walsky et al., 2012). PF-06409577 displayed weak inhibition of the major hepatic UGT isozymes with the most potent inhibitory

TABLE 2

Enzyme kinetic parameters and RAF values of PF-06409577 glucuronidation based on M1 formation in the presence of 2% BSA

The unbound fraction in incubation (PF-06409577) = 0.098. The V$_{max}$ and K$_M$ values in HLM, HIM, and hrUGT1A1 were calculated from eq. 3. The V$_{max}$ and K$_M$ values in HKM were calculated from eq. 1.

Parameter	HLM	HIM	HKM	hrUGT1A1
V_{max} (pmol/min per milligram)	2589 ± 93	718.9 ± 19	106.7 ± 1.8	3834 ± 77
K_M (μM)	184.4 ± 16	212.3 ± 13	116.4 ± 6.3	130.7 ± 7.5
h	1.76 ± 0.15	1.62 ± 0.081	N.A.	2.63 ± 0.27
CL$_{int}$ (μl/min per milligram)	7.09	1.74	0.917	15.1
CL$_{int,u}$ (μl/min per milligram)	72.3	17.8	9.35	154
RAF	0.47	0.12	0.061	N.A.

h, Hill coefficient; N.A., not applicable.

TABLE 3

Enzyme kinetic parameters and RAF values of ES glucuronidation based on ES-3-G formation in the presence of 2% BSA

The unbound fraction in incubation (ES) = 0.04. The V_{max} and K_M values in HLM and hrUGT1A1 were calculated from eq. 3. The V_{max} and K_M values in HIM and HKM were calculated from eq. 2.

Parameter	HLM	HIM	HKM	hrUGT1A1
V_{max} (pmol/min per milligram)	1522 ± 93	7095 ± 130	30.6 ± 2.6	2082 ± 45
K_M (μM)	147 ± 22	31.0 ± 1.4	18.7 ± 5.0	137 ± 8
h	1.61 ± 0.26	N.A.	N.A.	1.84 ± 0.13
CL_{int} (μl/min per milligram)	5.3	229	1.6	7.7
$CL_{int,u}$ (μl/min per milligram)	134	5720	41	192
RAF	0.7	30	0.22	N.A.

h, Hill coefficient; N.A., not applicable.

effects on the UGT1A1-catalyzed glucuronidation of ES to ES-3-G ($IC_{50} = 24$ μM) and the UGT1A9-catalyzed glucuronidation of propofol to propofol-O-glucuronide ($IC_{50} = 41.3$ μM) (Table 4). Under these experimental conditions, ES was evaluated as an inhibitor of the UGT2B7-catalyzed glucuronidation of AZT to zidovudine-5′-glucuronide in HLM. In addition to the known inhibitory effects against UGT1A1 (Nakajima et al., 2002; Watanabe et al., 2002, 2003; Mano et al., 2004, 2006; Katoh et al., 2007; Luo et al., 2012; Uchihashi et al., 2011; Seo et al., 2014) and UGT1A9 (Mano et al., 2004; Seo et al., 2014), we noted potent inhibition of UGT2B7 enzyme activity by ES with an IC_{50} value of 4.37 μM.

Discussion

Overlapping substrate specificity is a characteristic trait of human UGTs with small molecule xenobiotics often subject to glucuronidation by multiple UGT isoforms in native tissue (e.g., liver and intestine) (Tukey and Strassburg, 2000). In contrast to this norm, several in vitro assays demonstrated that PF-06409577 was glucuronidated by UGT1A1 in a selective fashion. Genetic variability of UGT1A1 in relation to its role in bilirubin metabolism has been extensively studied (Bosma et al., 1994; Strassburg et al., 2008; Marques and Ikediobi, 2010). The most common UGT1A1 polymorphism resulting from insertion of a thymine-adenine dinucleotide in the TATA-box of the UGT1A1 promoter (referred to as UGT1A1*28) is associated with Gilbert's syndrome, a mild form of inherited unconjugated hyperbilirubinemia arising from impairment in bilirubin glucuronidation (Bosma et al., 1994, 1995). Altered pharmacokinetic profiles of drugs metabolized by UGT1A1 in the homo- or heterozygous UGT1A1*28 polymorphic population can also result in dose-limiting toxicities such as the severe diarrhea and neutropenia noted with irinotecan (https://www.accessdata.fda.gov/drugsatfda_docs/label/2014/020571s048lbl.pdf). While the precise mechanism for irinotecan toxicity remains unclear, it is widely accepted that decreased UGT1A1 activity leads to elevated systemic levels of SN-38 (the hydrolytic cleavage product and active form of irinotecan), which is metabolically eliminated via glucuronidation by UGT1A1 (Iyer et al., 1998, 2002; Nagar and Blanchard, 2006). The hypothesis is consistent with the 50%–80% decrease in SN-38 glucuronidation in HLM UGT1A1*28 (Iyer et al., 1999; Gagné et al., 2002; Zhang et al., 2007). The observed correlation between genotype and clinical toxicity has led to the recommendation that patients are genotyped for the UGT1A1*28 polymorphism and dose adjustments are made before treatment with irinotecan (https://www.accessdata.fda.gov/drugsatfda_docs/label/2014/020571s048lbl.pdf). A second example of a marketed drug that requires dose adjustment in a UGT1A1*28 population is the hydroxamic acid derivative belinostat, which is cleared via glucuronidation by UGT1A1 (Wang et al., 2013). Significant increases in belinostat exposure and increased thrombocytopenia incidences in
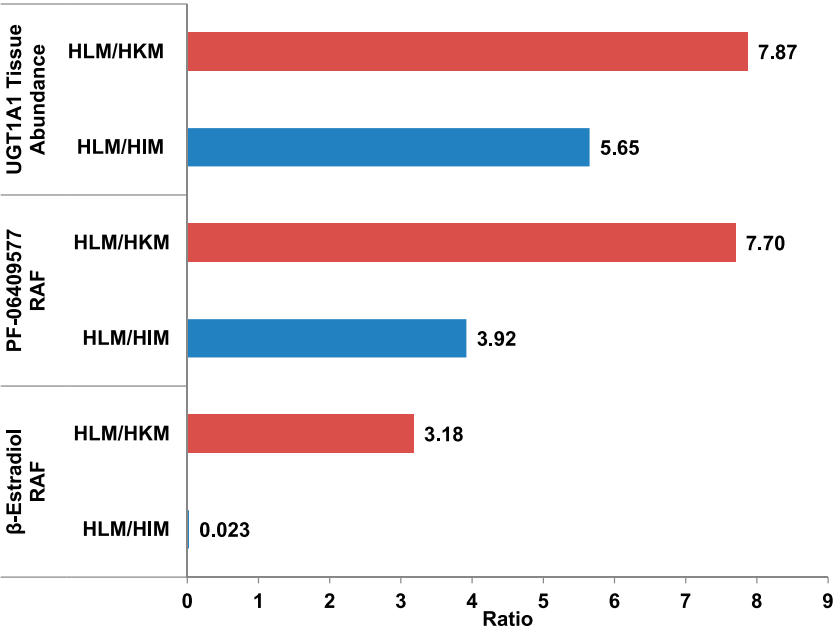
Fig. 5. Comparison of UGT1A1 tissue abundance ratios for HLM/HKM (red bar) and HLM/HIM (blue bar) to RAF ratios generated using PF-06409577 or ES as the probe substrate.
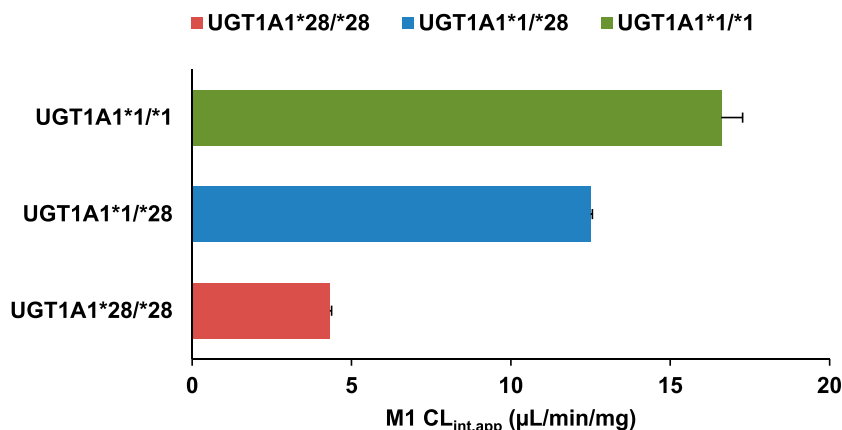
Fig. 6. Determination of the CL_{int} value for glucuronidation of PF-06409577 (1 μM) in pooled UGT1A1*1/*1 wild-type, heterozygote *1/*28, and homozygote *28/*28 HLM.

cancer patients harboring the UGT1A1*28 allele (Goey et al., 2016; Peer et al., 2016) are consistent with ~50% lower belinostat glucuronidation in UGT1A1*28 HLM.

The UGT1A1 substrate specificity of PF-06409577 has great significance from a clinical standpoint since first-in-human pharmacokinetics studies on PF-06409577 revealed that the parent compound and M1 were the only entities in circulation with a M1/PF-06409577 ratio of ~0.7–1.2 across a 3–30 mg dose range (Pfizer clinical data on file). The clinical development plan for PF-06409577 will require additional scrutiny with respect to potential alterations in pharmacokinetics, pharmacodynamics, and toxicological profile in patients harboring the UGT1A1*28 allele and in pharmacokinetic interaction studies with UGT1A1 inhibitors.

Our work also raises the possibility of utilizing PF-06409577 as a more selective UGT1A1 probe substrate in preclinical discovery. The kinetic parameters for glucuronidation of PF-06409577 and prototypic substrate ES were comparable in hrUGT1A1 incubations. However, assessment of UGT specificity with 13 hrUGTs revealed that PF-06409577 was considerably more selective as a UGT1A1 substrate in comparison with ES across a concentration range bracketing their respective K_M values. Besides UGT1A1, ES was also subject to glucuronidation by UGT1A3, 1A8, and 1A10. These observations are consistent with previous reports (Lépine et al., 2004; Itäaho et al., 2008)

in which multiple UGTs (1A3, 1A4, 1A8, 1A10, 2B7, and 2B15) catalyze the glucuronidation of ES, in addition to UGT1A1. The overlap in UGT substrate specificity for ES will compromise interpretation of in vitro data, particularly in human intestinal and kidney microsomal tissues, which express UGT1A isoforms (Cheng et al., 1999). Contributions of individual UGTs to a glucuronidation reaction in tissue microsomes can be estimated via the RAF method, originally developed to reflect differences between recombinant cytochrome P450 enzymes and HLM (Crespi and Miller, 1999), and recently extended to include UGTs (Rouguieg et al., 2010). Given the greater selectivity of PF-06409577 as a UGT1A1 substrate (relative to ES) in hrUGT assays, we decided to compare the corresponding RAF values with PF-06409577 and ES for liver, intestine, and kidney based on $CL_{int,u}$ values obtained in hrUGT1A1, HLM, HIM, and HKM. The RAF values in HLM and HKM for PF-06409577 and ES were less than unity, suggesting that hrUGT1A1 has much higher activity than native hepatic or kidney UGT1A1. The less than unity RAF value for UGT1A1 activity in HLM has been noted previously for various UGT1A1 substrates such as ES, SN-38, and etoposide (Rouguieg et al., 2010; Xiao et al., 2018).

The RAF values with PF-06409577 were generally consistent with UGT1A1 abundance in the small intestine, liver, and kidney. Furthermore, the RAF values for HLM and HKM were comparable between ES and PF-06409577 ($\pm$3-fold), which is expected since both compounds
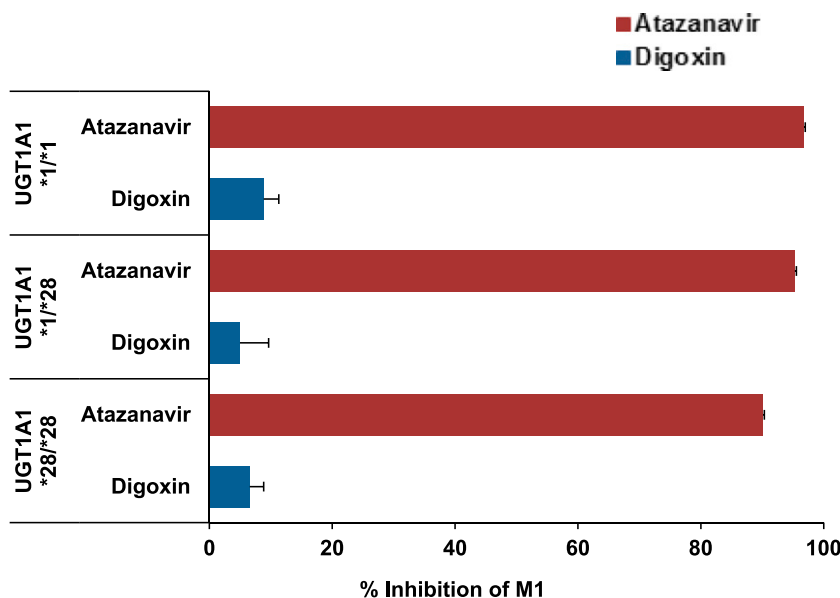

Fig. 7. Impact of selective UGT1A1 (atazanavir) and UGT1A9 (digoxin) inhibitors on the glucuronidation of PF-06409577 (1 μM) to M1 in pooled UGT1A1*1/*1 wild-type, heterozygote *1/*28, and homozygote *28/*28 HLM. Percentage of inhibition of M1 was normalized to the control activity for each genotype (*1/*1, *1/*28, and *28/*28).

TABLE 4

Inhibition of UGT by PF-06409577 and ES in the absence of 2% BSA

The ES UGT1A1 HLM IC$_{50}$ values used the following probe substrates: 5-(4-hydroxyphenyl)-5-phenylhydantoin, bergenin, etoposide, niflumic acid, puerarin, raltegravir, T5224, and troglitazone. The ES hrUGT1A9 IC$_{50}$ values were generated using 4-methylumbelliferone and scopoletin as the probe substrate.

UGT Isoform	PF-06409577 C$_{50}$ and 95% CI μM	ES IC$_{50}$ and 95% CI μM
1A1	24 (20.6–27.2)	4.21–261[a]
1A4	>100	N.D.
1A6	>100	N.D.
1A9	41.3 (30.5–55.9)	2.1[a]
2B7	>100	4.37 (3.97–4.80)

CI, confidence interval; N.D., not determined.

[a]The IC$_{50}$ values were obtained from the University of Washington Drug Interaction Database (https://didb.druginteractioninfo.org/query/enzyme/precipitants-affecting-enzyme/?QueryId=12&EnzymeOid=82&EffectId=0).

are selectively metabolized by UGT1A1 in the liver and kidney. In contrast, the RAF values for HIM varied depending on the substrate used; the ES HIM RAF was 30, whereas the PF-06409577 RAF was 0.12. This 250-fold discrepancy, which is also reflected in the UGT1A1 intestinal abundance data (ES RAF HLM/HIM 0.023 vs. UGT1A1 abundance liver/intestine 5.7), suggests that intestinal UGT1A8 and UGT1A10 contribute toward ES glucuronidation, while PF-06409577 is relatively latent toward glucuronidation by these UGTs. Consequently, ES glucuronidation activity in HIM is the culmination of all three UGT isoforms (UGT1A1, 1A8, and 1A10), and therefore an overestimation of UGT1A1 activity. These data also suggest that relative to UGT1A1, UGT1A8 and 1A10 are the major UGT isoforms responsible for ES-3-G formation in the gut, considering the similar abundance of these UGTs in the intestine (SIMCYP database). Conversely, PF-06409577, which is not a substrate for UGT1A8 and 1A10, resulted in a lower RAF value in HIM. Based on our findings, we recommend using PF-06409577 to determine RAF values for scaling hrUGT1A1 activity to intestinal glucuronidation since the ES RAF value would likely result in an overprediction due to contributions of other UGT isoforms.

An additional advantage lies in the utility of PF-06409577 as a specific UGT1A1 substrate in UGT inhibition studies. Assessment of the inhibitory potential of new chemical entities against major human UGT isoforms from the UGT1A and UGT2B families in HLM often relies on a cocktail assay in the presence of multiple probe UGT substrates, which have been shown as specific for individual UGT isoforms in a single incubation (Joo et al., 2014; Seo et al., 2014; Gradinaru et al., 2015; Lee at al., 2015). Several compounds, including bilirubin, ES, SN-38 (Lee et al., 2015), and etoposide have been used as in vitro probe substrates for UGT1A1. Because of the challenges associated with separation and simultaneous determination of the multiple glucuronide isomers formed with bilirubin (Zhang et al., 2005) and etoposide (Watanabe et al., 2003; Wen et al., 2007; Gradinaru et al., 2015), ES is routinely used to characterize UGT1A1 inhibition with the understanding that other UGTs will contribute to its metabolism. Besides UGT1A1, there are several reports on SN-38 glucuronidation by members of the UGT1A family (Iyer et al., 1998; Hanioka et al., 2001; Gagné et al., 2002; Tallman et al., 2005; Zhang et al., 2007). Recently, Xiao et al. (2018) have provided convincing evidence suggesting that UGT1A9 and UGT1A1 contribute equally to SN-38 glucuronidation in HLM. Consistent with this in vitro observation, clinical studies also demonstrated that UGT1A9 polymorphism acted as an additional biomarker of irinotecan toxicities (Girard et al., 2006; Sandanaraj et al., 2008). Furthermore, in cocktail HLM incubations, it is noteworthy to point out that the activities of individual UGT isoforms can be inhibited by the UGT substrate cocktail. For example,

ES is a UGT1A1 substrate as well as a potent inhibitor of UGT1A1 activity. The inhibition data generated in our present study also demonstrated potent inhibition of UGT2B7 activity by ES in HLM with an IC$_{50}$ value of 4.37 μM. In contrast to these findings, PF-06409577 demonstrated little-to-no inhibition of UGT1A4, 1A6, and 2B7 isoforms, with the most potent inhibitory effects being against UGT1A1 (IC$_{50}$ = 24 μM) and UGT1A9 (IC$_{50}$ = 41.3 μM). Based on this observation, we have replaced ES with PF-06409577 as a probe UGT1A1 substrate in our HLM cocktail UGT inhibition assay to examine UGT1A1, 1A9, and 2B7 inhibitory potential of new chemical entities in preclinical discovery. The IC$_{50}$ values for literature UGT1A1 inhibitors are comparable when using either PF-06409577 or ES as probe substrates (unpublished data).

Finally, in the absence of human UGT crystal structures, information regarding molecular determinants that govern substrate specificity toward individual UGT isoforms remains elusive. The chemical space encompassing selective UGT1A1 substrate matter is structurally diverse with significant differences in physiochemical properties [e.g., PF-06409577 (molecular weight = 341; clogP = 4.42), SN-38 (molecular weight = 392; clogP = 1.67), belinostat (molecular weight = 318; clogP = 1.17), etoposide (molecular weight = 588; clogP = −0.1), and bilirubin (molecular weight = 584; clogP = 3.21)]. Pharmacophore modeling and quantitative structure-activity relationship studies suggest that specificity toward glucuronidation by UGT1A1 is governed by two hydrophobic domains ~4 and 7 Å, respectively, from the site of glucuronidation (Sorich et al., 2002). Studies are currently underway to test and further refine this hypothesis using the literature UGT1A1-selective substrates discussed in this paper as well as chemical lead matter from the indole-3-carboxylic acid series of AMPK activators, with the hope of identifying backup candidates with reduced UGT1A1 substrate specificity.

Authorship Contributions

Participated in research design: Kalgutkar, Lapham, Goosen, Lin, Di.

Conducted experiments: Lapham, Novak, Niosi, Orozco, Lin, Eng, Ryu, Riccardi.

Contributed new reagents or analytic tools: Cameron.

Performed data analysis: Lapham, Novak, Niosi, Orozco, Lin, Eng, Goosen, Di, Kalgutkar.

Wrote or contributed to the writing of the manuscript: Kalgutkar, Lapham, Novak, Niosi, Orozco, Lin, Eng, Goosen, Di.

References

Argikar UA (2012) Unusual glucuronides. *Drug Metab Dispos* **40**:1239–1251.

Beutler E, Gelbart T, and Demina A (1998) Racial variability in the UDP-glucuronosyltransferase 1 (UGT1A1) promoter: a balanced polymorphism for regulation of bilirubin metabolism? *Proc Natl Acad Sci USA* **95**:8170–8174.

Bjornsson TD, Callaghan JT, Einolf HJ, Fischer V, Gan L, Grimm S, Kao J, King SP, Miwa G, Ni L, et al.; Pharmaceutical Research and Manufacturers of America (PhRMA) Drug Metabolism/Clinical Pharmacology Technical Working Group; FDA Center for Drug Evaluation and Research (CDER) (2003) The conduct of in vitro and in vivo drug-drug interaction studies: a Pharmaceutical Research and Manufacturers of America (PhRMA) perspective. *Drug Metab Dispos* **31**:815–832.

Bosma PJ, Chowdhury JR, Bakker C, Gantla S, de Boer A, Oostra BA, Lindhout D, Tytgat GN, Jansen PL, Oude Elferink RP, et al. (1995) The genetic basis of the reduced expression of bilirubin UDP-glucuronosyltransferase 1 in Gilbert's syndrome. *N Engl J Med* **333**:1171–1175.

Bosma PJ, Seppen J, Goldhoorn B, Bakker C, Oude Elferink RP, Chowdhury JR, Chowdhury NR, and Jansen PL (1994) Bilirubin UDP-glucuronosyltransferase 1 is the only relevant bilirubin glucuronidating isoform in man. *J Biol Chem* **269**:17960–17964.

Cameron KO, Kung DW, Kalgutkar AS, Kurumbail RG, Miller R, Salatto CT, Ward J, Withka JM, Bhattacharya SK, Boehm M, et al. (2016) Discovery and preclinical characterization of 6-chloro-5-[4-(1-hydroxycyclobutyl)phenyl]-1*H*-indole-3-carboxylic acid (PF-06409577), a direct activator of adenosine monophosphate-activated protein kinase (AMPK), for the potential treatment of diabetic nephropathy. *J Med Chem* **59**:8068–8081.

Cheng Z, Radominska-Pandya A, and Tephly TR (1999) Studies on the substrate specificity of human intestinal UDP-lucuronosyltransferases 1A8 and 1A10. *Drug Metab Dispos* **27**:1165–1170.

Court MH (2010) Interindividual variability in hepatic drug glucuronidation: studies into the role of age, sex, enzyme inducers, and genetic polymorphism using the human liver bank as a model system. *Drug Metab Rev* 42:209–224.

Crespi CL and Miller VP (1999) The use of heterologously expressed drug metabolizing enzymes—state of the art and prospects for the future. *Pharmacol Ther* 84:121–131.

Devineni D, Vaccaro N, Murphy J, Curtin C, Mamidi RN, Weiner S, Wang SS, Ariyawansa J, Stieltjes H, Wajs E, et al. (2015) Effects of rifampin, cyclosporine A, and probenecid on the pharmacokinetic profile of canagliflozin, a sodium glucose co-transporter 2 inhibitor, in healthy participants. *Int J Clin Pharmacol Ther* 53:115–128.

Di L, Keefer C, Scott DO, Strelevitz TJ, Chang G, Bi YA, Lai Y, Duckworth J, Fenner K, Troutman MD, et al. (2012) Mechanistic insights from comparing intrinsic clearance values between human liver microsomes and hepatocytes to guide drug design. *Eur J Med Chem* 57:441–448.

Duguay Y, McGrath M, Lépine J, Gagné JF, Hankinson SE, Colditz GA, Hunter DJ, Plante M, Têtu B, Bélanger A, et al. (2004) The functional UGT1A1 promoter polymorphism decreases endometrial cancer risk. *Cancer Res* 64:1202–1207.

Engtrakul JJ, Foti RS, Strelevitz TJ, and Fisher MB (2005) Altered AZT (3′-azido-3′-deoxythymidine) glucuronidation kinetics in liver microsomes as an explanation for underprediction of in vivo clearance: comparison to hepatocytes and effect of incubation environment. *Drug Metab Dispos* 33:1621–1627.

Fisher MB, Paine MF, Strelevitz TJ, and Wrighton SA (2001) The role of hepatic and extrahepatic UDP-glucuronosyltransferases in human drug metabolism. *Drug Metab Rev* 33:273–297.

Fujiwara R, Maruo Y, Chen S, and Tukey RH (2015) Role of extrahepatic UDP-glucuronosyltransferase 1A1: advances in understanding breast milk-induced neonatal hyperbilirubinemia. *Toxicol Appl Pharmacol* 289:124–132.

Gagné JF, Montminy V, Belanger P, Journault K, Gaucher G, and Guillemette C (2002) Common human UGT1A polymorphisms and the altered metabolism of irinotecan active metabolite 7-ethyl-10-hydroxycamptothecin (SN-38). *Mol Pharmacol* 62:608–617.

Gibson CR, Lu P, Maciolek C, Wudarski C, Barter Z, Rowland-Yeo K, Stroh M, Lai E, and Nicoll-Griffith DA (2013) Using human recombinant UDP-glucuronosyltransferase isoforms and a relative activity factor approach to model total body clearance of laropiprant (MK-0524) in humans. *Xenobiotica* 43:1027–1036.

Girard H, Villeneuve L, Court MH, Fortier LC, Caron P, Hao Q, von Moltke LL, Greenblatt DJ, and Guillemette C (2006) The novel UGT1A9 intronic I399 polymorphism appears as a predictor of 7-ethyl-10-hydroxycamptothecin glucuronidation levels in the liver. *Drug Metab Dispos* 34:1220–1228.

Goey AK, Sissung TM, Peer CJ, Trepel JB, Lee MJ, Tomita Y, Ehrlich S, Bryla C, Balasubramaniam S, Piekarz R, et al. (2016) Effects of UGT1A1 genotype on the pharmacokinetics, pharmacodynamics, and toxicities of belinostat administered by 48-hour continuous infusion in patients with cancer. *J Clin Pharmacol* 56:461–473.

Gradinaru J, Romand S, Geiser L, Carrupt PA, Spaggiari D, and Rudaz S (2015) Inhibition screening method of microsomal UGTs using the cocktail approach. *Eur J Pharm Sci* 71:35–45.

Hanioka N, Ozawa S, Jinno H, Ando M, Saito Y, and Sawada J (2001) Human liver UDP-glucuronosyltransferase isoforms involved in the glucuronidation of 7-ethyl-10-hydroxycamptothecin. *Xenobiotica* 31:687–699.

Harbourt DE, Fallon JK, Ito S, Baba T, Ritter JK, Glish GL, and Smith PC (2012) Quantification of human uridine-diphosphate glucuronosyl transferase 1A isoforms in liver, intestine, and kidney using nanobore liquid chromatography-tandem mass spectrometry. *Anal Chem* 84:98–105.

Hawes EM (1998) N^+-glucuronidation, a common pathway in human metabolism of drugs with a tertiary amine group. *Drug Metab Dispos* 26:830–837.

Hu DG, Meech R, McKinnon RA, and Mackenzie PI (2014) Transcriptional regulation of human UDP-glucuronosyltransferase genes. *Drug Metab Rev* 46:421–458.

Itäaho K, Mackenzie PI, Ikushiro S, Miners JO, and Finel M (2008) The configuration of the 17-hydroxy group variably influences the glucuronidation of β-estradiol and epiestradiol by human UDP-glucuronosyltransferases. *Drug Metab Dispos* 36:2307–2315.

Iyer L, Das S, Janisch L, Wen M, Ramírez J, Karrison T, Fleming GF, Vokes EE, Schilsky RL, and Ratain MJ (2002) UGT1A1*28 polymorphism as a determinant of irinotecan disposition and toxicity. *Pharmacogenomics J* 2:43–47.

Iyer L, Hall D, Das S, Mortell MA, Ramírez J, Kim S, Di Rienzo A, and Ratain MJ (1999) Phenotype-genotype correlation of in vitro SN-38 (active metabolite of irinotecan) and bilirubin glucuronidation in human liver tissue with UGT1A1 promoter polymorphism. *Clin Pharmacol Ther* 65:576–582.

Iyer L, King CD, Whitington PF, Green MD, Roy SK, Tephly TR, Coffman BL, and Ratain MJ (1998) Genetic predisposition to the metabolism of irinotecan (CPT-11). Role of uridine diphosphate glucuronosyltransferase isoform 1A1 in the glucuronidation of its active metabolite (SN-38) in human liver microsomes. *J Clin Invest* 101:847–854.

Joo J, Lee B, Lee T, and Liu KH (2014) Screening of six UGT enzyme activities in human liver microsomes using liquid chromatography/triple quadrupole mass spectrometry. *Rapid Commun Mass Spectrom* 28:2405–2414.

Kaivosaari S, Finel M, and Koskinen M (2011) *N*-glucuronidation of drugs and other xenobiotics by human and animal UDP-glucuronosyltransferases. *Xenobiotica* 41:652–669.

Katoh M, Matsui T, and Yokoi T (2007) Glucuronidation of antiallergic drug, Tranilast: identification of human UDP-glucuronosyltransferase isoforms and effect of its phase I metabolite. *Drug Metab Dispos* 35:583–589.

Kiang TK, Ensom MH, and Chang TK (2005) UDP-glucuronosyltransferases and clinical drug-drug interactions. *Pharmacol Ther* 106:97–132.

Krishna R, East L, Larson P, Siringhaus T, Herpok L, Bethel-Brown C, Manthos H, Brejda J, and Gartner M (2016) Efavirenz does not meaningfully affect the single dose pharmacokinetics of 1200 mg raltegravir. *Biopharm Drug Dispos* 37:542–549.

Lapham K, Bauman JN, Walsky RL, Bourcier K, Giddens G, Obach RS, Hyland R, and Goosen TC (2012) Digoxin and tranilast identified as novel isoform-selective inhibitors of human UDP glucuronosyltransferase 1A9 (UGT1A9) activity (P108). *Drug Metab Rev* 44:82.

Lee B, Ji HK, Lee T, and Liu KH (2015) Simultaneous screening of activities of five cytochrome P450 and four uridine 5′-diphospho-glucuronosyltransferase enzymes in human liver microsomes using cocktail incubation and liquid chromatography–tandem mass spectrometry. *Drug Metab Dispos* 43:1137–1146.

Lépine J, Bernard O, Plante M, Têtu B, Pelletier G, Labrie F, Bélanger A, and Guillemette C (2004) Specificity and regioselectivity of the conjugation of estradiol, estrone, and their catecholestrogen and methoxyestrogen metabolites by human uridine diphospho-glucuronosyltransferases expressed in endometrium. *J Clin Endocrinol Metab* 89:5222–5232.

Luo CF, Cai B, Hou N, Yuan M, Liu SM, Ji H, Xiong LG, Xiong W, Luo JD, and Chen MS (2012) UDP-glucuronosyltransferase 1A1 is the principal enzyme responsible for puerarin metabolism in human liver microsomes. *Arch Toxicol* 86:1681–1690.

Mackenzie PI, Owens IS, Burchell B, Bock KW, Bairoch A, Bélanger A, Fournel-Gigleux S, Green M, Hum DW, Iyanagi T, et al. (1997) The UDP glycosyltransferase gene superfamily: recommended nomenclature update based on evolutionary divergence. *Pharmacogenetics* 7:255–269.

Mano Y, Usui T, and Kamimura H (2004) Effects of β-estradiol and propofol on the 4-methylumbelliferone glucuronidation in recombinant human UGT isozymes 1A1, 1A8 and 1A9. *Biopharm Drug Dispos* 25:339–344.

Mano Y, Usui T, and Kamimura H (2006) Identification of human UDP-glucuronosyltransferase responsible for the glucuronidation of niflumic acid in human liver. *Pharm Res* 23:1502–1508.

Marques SC and Ikediobi ON (2010) The clinical application of UGT1A1 pharmacogenetic testing: gene-environment interactions. *Hum Genomics* 4:238–249.

Miners JO and Mackenzie PI (1991) Drug glucuronidation in humans. *Pharmacol Ther* 51:347–369.

Nagar S and Blanchard RL (2006) Pharmacogenetics of uridine diphosphoglucuronosyltransferase (UGT) 1A family members and its role in patient response to irinotecan. *Drug Metab Rev* 38:393–409.

Nakajima M, Sakata N, Ohashi N, Kume T, and Yokoi T (2002) Involvement of multiple UDP-glucuronosyltransferase 1A isoforms in glucuronidation of 5-(4′-hydroxyphenyl)-5-phenylhydantoin in human liver microsomes. *Drug Metab Dispos* 30:1250–1256.

Ohno S and Nakajin S (2009) Determination of mRNA expression of human UDP-glucuronosyltransferases and application for localization in various human tissues by real-time reverse transcriptase-polymerase chain reaction. *Drug Metab Dispos* 37:32–40.

Peer CJ, Goey AK, Sissung TM, Erlich S, Lee MJ, Tomita Y, Trepel JB, Piekarz R, Balasubramaniam S, Bates SE, et al. (2016) UGT1A1 genotype-dependent dose adjustment of belinostat in patients with advanced cancers using population pharmacokinetic modeling and simulation. *J Clin Pharmacol* 56:450–460.

Rouguieg K, Picard N, Sauvage FL, Gaulier JM, and Marquet P (2010) Contribution of the different UDP-glucuronosyltransferase (UGT) isoforms to buprenorphine and norbuprenorphine metabolism and relationship with the main UGT polymorphisms in a bank of human liver microsomes. *Drug Metab Dispos* 38:40–45.

Rowland A, Gaganis P, Elliot DJ, Mackenzie PI, Knights KM, and Miners JO (2007) Binding of inhibitory fatty acids is responsible for the enhancement of UDP-glucuronosyltransferase 2B7 activity by albumin: implications for in vitro-in vivo extrapolation. *J Pharmacol Exp Ther* 321:137–147.

Rowland A, Knights KM, Mackenzie PI, and Miners JO (2008) The "albumin effect" and drug glucuronidation: bovine serum albumin and fatty acid-free human serum albumin enhance the glucuronidation of UDP-glucuronosyltransferase (UGT) 1A9 substrates but not UGT1A1 and UGT1A6 activities. *Drug Metab Dispos* 36:1056–1062.

Ryder TF, Calabrese MF, Walker GS, Cameron KO, Reyes AR, Borzilleri KA, Delmore J, Miller R, Kurumbail RG, Ward J, et al. (2018) Acyl glucuronide metabolites of 6-chloro-5-[4-(1-hydroxycyclobutyl)phenyl]-1*H*-indole-3-carboxylic acid (PF-06409577) and related indole-3-carboxylic acid derivatives are direct activators of adenosine monophosphate-activated protein kinase (AMPK). *J Med Chem* 61:7273–7288.

Sai K, Saeki M, Saito Y, Ozawa S, Katori N, Jinno H, Hasegawa R, Kaniwa N, Sawada J, Komamura K, et al. (2004) UGT1A1 haplotypes associated with reduced glucuronidation and increased serum bilirubin in irinotecan-administered Japanese patients with cancer. *Clin Pharmacol Ther* 75:501–515.

Sakaguchi K, Green M, Stock N, Reger TS, Zunic J, and King C (2004) Glucuronidation of carboxylic acid containing compounds by UDP-glucuronosyltransferase isoforms. *Arch Biochem Biophys* 424:219–225.

Sandanaraj E, Jada SR, Shu X, Lim R, Lee SC, Zhou Q, Zhou S, Goh BC, and Chowbay B (2008) Influence of UGT1A9 intronic I399C>T polymorphism on SN-38 glucuronidation in Asian cancer patients. *Pharmacogenomics J* 8:174–185.

Seo KA, Kim HJ, Jeong ES, Abdalla N, Choi CS, Kim DH, and Shin JG (2014) In vitro assay of six UDP-glucuronosyltransferase isoforms in human liver microsomes, using cocktails of probe substrates and liquid chromatography–tandem mass spectrometry. *Drug Metab Dispos* 42:1803–1810.

Sorich MJ, Smith PA, McKinnon RA, and Miners JO (2002) Pharmacophore and quantitative structure activity relationship modelling of UDP-glucuronosyltransferase 1A1 (UGT1A1) substrates. *Pharmacogenetics* 12:635–645.

Strassburg CP, Lankisch TO, Manns MP, and Ehmer U (2008) Family 1 uridine-5′-diphosphate glucuronosyltransferases (UGT1A): from Gilbert's syndrome to genetic organization and variability. *Arch Toxicol* 82:415–433.

Sugatani J (2013) Function, genetic polymorphism, and transcriptional regulation of human UDP-glucuronosyltransferase (UGT) 1A1. *Drug Metab Pharmacokinet* 28:83–92.

Tallman MN, Ritter JK, and Smith PC (2005) Differential rates of glucuronidation for 7-ethyl-10-hydroxy-camptothecin (SN-38) lactone and carboxylate in human and rat microsomes and recombinant UDP-glucuronosyltransferase isoforms. *Drug Metab Dispos* 33:977–983.

Toffoli G, Cecchin E, Corona G, Russo A, Buonadonna A, D'Andrea M, Pasetto LM, Pessa S, Errante D, De Pangher V, et al. (2006) The role of UGT1A1*28 polymorphism in the pharmacodynamics and pharmacokinetics of irinotecan in patients with metastatic colorectal cancer. *J Clin Oncol* 24:3061–3068.

Tsoutsikos P, Miners JO, Stapleton A, Thomas A, Sallustio BC, and Knights KM (2004) Evidence that unsaturated fatty acids are potent inhibitors of renal UDP-glucuronosyltransferases (UGT): kinetic studies using human kidney cortical microsomes and recombinant UGT1A9 and UGT2B7. *Biochem Pharmacol* 67:191–199.

Tukey RH and Strassburg CP (2000) Human UDP-glucuronosyltransferases: metabolism, expression, and disease. *Annu Rev Pharmacol Toxicol* 40:581–616.

Tukey RH and Strassburg CP (2001) Genetic multiplicity of the human UDP-glucuronosyltransferases and regulation in the gastrointestinal tract. *Mol Pharmacol* 59:405–414.

Uchihashi S, Fukumoto H, Onoda M, Hayakawa H, Ikushiro S, and Sakaki T (2011) Metabolism of the c-Fos/activator protein-1 inhibitor T-5224 by multiple human UDP-glucuronosyltransferase isoforms. *Drug Metab Dispos* 39:803–813.

Walsky RL, Bauman JN, Bourcier K, Giddens G, Lapham K, Negahban A, Ryder TF, Obach RS, Hyland R, and Goosen TC (2012) Optimized assays for human UDP-glucuronosyltransferase

(UGT) activities: altered alamethicin concentration and utility to screen for UGT inhibitors. *Drug Metab Dispos* **40**:1051–1065.

Wang LZ, Ramírez J, Yeo W, Chan MY, Thuya WL, Lau JY, Wan SC, Wong AL, Zee YK, Lim R, et al. (2013) Glucuronidation by UGT1A1 is the dominant pathway of the metabolic disposition of belinostat in liver cancer patients. *PLoS One* **8**:e54522.

Watanabe Y, Nakajima M, Ohashi N, Kume T, and Yokoi T (2003) Glucuronidation of etoposide in human liver microsomes is specifically catalyzed by UDP-glucuronosyltransferase 1A1. *Drug Metab Dispos* **31**:589–595.

Watanabe Y, Nakajima M, and Yokoi T (2002) Troglitazone glucuronidation in human liver and intestine microsomes: high catalytic activity of UGT1A8 and UGT1A10. *Drug Metab Dispos* **30**:1462–1469.

Wen Z, Tallman MN, Ali SY, and Smith PC (2007) UDP-glucuronosyltransferase 1A1 is the principal enzyme responsible for etoposide glucuronidation in human liver and intestinal microsomes: structural characterization of phenolic and alcoholic glucuronides of etoposide and estimation of enzyme kinetics. *Drug Metab Dispos* **35**:371–380.

Xiao L, Zhu L, Li W, Li C, Cao Y, Ge G, and Sun X (2018) New insights into SN-38 glucuronidation: evidence for the important role of UDP glucuronosyltransferase 1A9. *Basic Clin Pharmacol Toxicol* **122**:424–428.

Zhang D, Chando TJ, Everett DW, Patten CJ, Dehal SS, and Humphreys WG (2005) In vitro inhibition of UDP glucuronosyltransferases by atazanavir and other HIV protease inhibitors and the relationship of this property to in vivo bilirubin glucuronidation. *Drug Metab Dispos* **33**:1729–1739.

Zhang D, Zhang D, Cui D, Gambardella J, Ma L, Barros A, Wang L, Fu Y, Rahematpura S, Nielsen J, et al. (2007) Characterization of the UDP glucuronosyltransferase activity of human liver microsomes genotyped for the *UGT1A1*28* polymorphism. *Drug Metab Dispos* **35**:2270–2280.

Zhang L, Reynolds KS, Zhao P, and Huang SM (2010) Drug interactions evaluation: an integrated part of risk assessment of therapeutics. *Toxicol Appl Pharmacol* **243**:134–145.

Zhu L, Ge G, Zhang H, Liu H, He G, Liang S, Zhang Y, Fang Z, Dong P, Finel M, et al. (2012) Characterization of hepatic and intestinal glucuronidation of magnolol: application of the relative activity factor approach to decipher the contributions of multiple UDP-glucuronosyltransferase isoforms. *Drug Metab Dispos* **40**:529–538.

Address correspondence to: Amit S. Kalgutkar, Medicine Design, Pfizer Inc., 1 Portland Street, Cambridge, MA 02139. E-mail: amit.kalgutkar@pfizer.com; or Kimberly Lapham, Medicine Design, Pfizer Inc., Eastern Point Road, Groton, CT 06340. E-mail: kimberly.lapham@pfizer.com